This is a post-peer-review, pre-copyedit version of an article published in the International Journal of Architectural Heritage, DOI: 10.1080/15583058.2018.1563226

TITLE: **DYNAMIC ONE-SIDED OUT-OF-PLANE BEHAVIOUR OF UNREINFORCED-MASONRY WALL RESTRAINED BY ELASTO-PLASTIC TIE-RODS**

AUTHORS

Omar AlShawa, Department of Structural and Geotechnical Engineering, via Antonio Gramsci 53, 00197 Roma, Italy, Ph.: + 39 06 4991 9155, Fax: +39 06 4991 9183, E-mail: omar.alshawa@uniroma1.it.(Corresponding author)

Domenico Liberatore, Department of Structural and Geotechnical Engineering, via Antonio Gramsci 53, 00197 Roma, Italy, Ph.: + 39 06 4991 9155, Fax: +39 06 4991 9183, E-mail: domenico.liberatore@uniroma1.it

Luigi Sorrentino, Department of Structural and Geotechnical Engineering, via Antonio Gramsci 53, 00197 Roma, Italy, Ph.: + 39 06 4991 9166, Fax: +39 06 4991 9183, E-mail: Luigi.sorrentino@uniroma1.it

ABSTRACT

Past earthquakes have shown the high vulnerability of existing masonry buildings, particularly to out-of-plane local collapse mechanisms. Such mechanisms can be prevented if façades are restrained by tie rods improving the connections to perpendiculars walls. Whereas in the past only static models have been proposed, herein the non-linear equation of motion of a monolithic wall restrained by a tie rod is presented. The façade, resting on a foundation and adjacent to transverse walls, rotates only around one base pivot and has one degree of freedom. Its thickness is explicitly accounted for and the tie rod is modelled as a linear elastic - perfectly plastic spring, with limited displacement capacity. The model is used to investigate the response to variations of wall geometry (height/thickness ratio, thickness), tie rod features (vertical position, length, prestress level), material characteristics (elastic modulus, ultimate elongation, yield strength) typical of historical iron. The most relevant parameter is the steel strength, whereas other characteristics play minor roles allowing to recommend reduced values for pre-tensioning forces. The force-based procedure customary in Italy for tie design is reasonably safe and involves protection also against collapse, although probably not enough as desirable.

KEYWORDS

rocking, historical iron, linear static procedure, prestress, steel, tie bar, ultimate elongation

RUNNING HEAD

Dynamic one-sided out-of-plane behaviour of unreinforced-masonry wall restrained by elasto-plastic tie rods

1 INTRODUCTION

Earthquakes have shown that unreinforced-masonry structures frequently present a higher vulnerability than reinforced-concrete structures (Zucconi, Ferlito, and Sorrentino 2017; Zucconi, Sorrentino, and Ferlito 2017), with out-of-plane loading being particularly dangerous if connections of façades to transversal structures are inadequate (Bruneau 1994; Brando et al. 2018; Moon et al. 2014; Mendes et al. 2017). Metal tie rods are among the most ancient details adopted to improve earthquake performance in unreinforced masonry buildings (Figure 1a), and their use is documented in several countries, such as Haiti (Rosenboom, Kelley, and Paret 2014), Italy (Sorrentino, Bruccoleri, and Antonini 2008; Lucibello et al. 2013; Gizzi et al. 2014), New Zealand (Campbell et al. 2012; Walsh et al. 2014; Marotta et al. 2015), and Turkey (Celik, Sesigur, and Cili 2009).

a) b)

Figure 1. Amatrice, Central Italy. a) Building strengthened by steel tie rods survived the 2016 earthquake, whereas nearby one collapsed, b) close up of wall anchor and permanent displacement of tie rod.

Steel ties have been recently proposed for cost-effective strengthening of both ordinary (Pomonis and Gaspari 2014) and monumental buildings (Degli Abbati et al. 2015). Shake table tests have proven their effectiveness in brickwork (Tomaževič, Lutman, and Weiss 1996) and natural stonework models (Magenes et al. 2014; Penna et al. 2016), provided that masonry disintegration does not occur (De Felice 2011; Liberatore et al. 2016). Vertical tendons and viscous dampers have been analytically investigated to control the response of rocking equipment and blocks (Makris and Zhang 2001; Dimitrakopoulos and DeJong 2012), and the use of superelastic alloys has been proposed for horizontal ties in the last decade (Indirli and Castellano 2008; Paret et al. 2008), but usually interventions are carried out with horizontal conventional-steel tie rods. Worked-out examples are available in books (Giuffrè 1993; Cangi, Caraboni, and De Maria 2010) and guidelines (Munari et al. 2010), but only static procedures are proposed without a proper validation by means of non-linear time-history analyses. Therefore, hereinafter a single-degree-of-freedom dynamic model of a monolithic wall restrained by a tie rod is presented. Although similar models have been proposed recently for a wall restrained at the top by a flexible diaphragm (Prajapati, AlShawa, and Sorrentino 2015; Giresini, Fragiacomo, and Lourenço 2015), the tie considered in the following is elasto-plastic, can fail if stretched beyond ultimate elongation and can be placed at any vertical position along the wall height. Moreover, its design is explicitly discussed and related parametric analyses are performed. The proposed model assumes that, as a result of a capacity design process, no failure at wall anchor (neither in the steel connection nor in the adjacent masonry) occurs and damage is concentrated in the easier-to-replace tie rod (Figure 1b). Finally, it is assumed that during motion no change in mechanism takes place, from single body to two bodies (Penner and Elwood 2016; Abrams et al. 2017), because the wall has a sufficiently low height/thickness ratio and because no openings are present that could further complicate the shape of the mechanism (Andreotti, Liberatore, and Sorrentino 2015; AlShawa, Sorrentino, and Liberatore 2017).

2 ANALYTICAL MODEL

In this section the dynamic model of a monolithic wall of finite thickness, free to rotate on one side only and restrained by an elasto-plastic tie having limited displacement capacity, is presented (Figure 2a). The model has two sources of non-linearity: wall geometry, involving a lever arm changing with rotation (Figure 2b), and tie rod material, becoming plastic if a yield displacement is overcome. The tie can be positioned at any height of the wall, friction is assumed to be large enough to prevent sliding both at the base and at wall anchor.

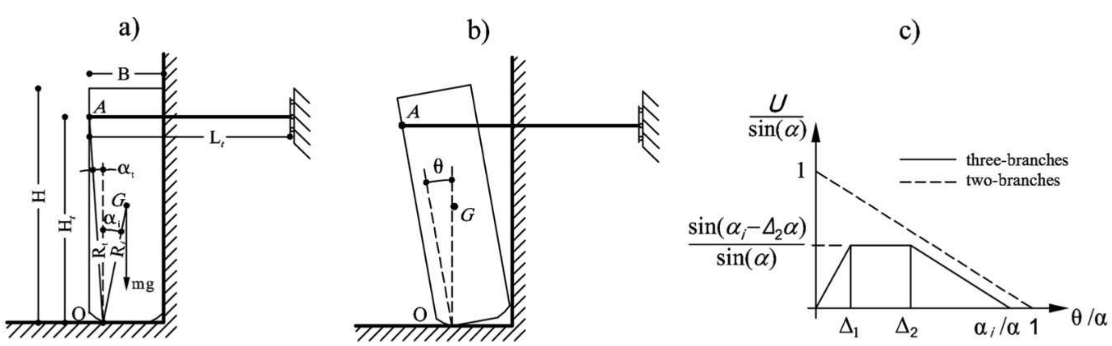

Figure 2. a) Geometrical parameters accounting for hinge indentation; b) One-sided displaced configuration ($\theta > 0$). c) Normalised self-weight restoring moment–rotation relationship.

Considering only positive rotations, the analytical equation of motion is the following:

$$\ddot{\theta} + \frac{p^2}{g}\left[\left(\ddot{y}_g + g\right)U(\theta, \alpha, \alpha_i, \Delta_1, \Delta_2) - \ddot{x}_g cos(\alpha_i - \theta) + \frac{\chi(\varepsilon_t)F_y R_t}{m\, R_i} cos(\alpha_t + \theta)\right] = 0 \qquad (1)$$

where θ = wall rotation (Figure 2b) and dot indicating derivative with respect to time, $p = \sqrt{mR_i g/I_O}$ = frequency parameter, m = mass of the wall, R_i = distance between centroid G and indented hinge O, g = gravity acceleration, I_O = polar moment of inertia of the wall with respect to O, $\ddot{x}_g$, $\ddot{y}_g$ = horizontal, vertical ground motion acceleration, U = non-dimensional wall-self-weight restoring moment parameter equal to:

$$U = \begin{cases} \dfrac{\theta}{\Delta_1 \alpha} sin(\alpha_i - \Delta_2 \alpha) & \theta \leq \Delta_1 \alpha \\ sin(\alpha_i - \Delta_2 \alpha) & \Delta_1 \alpha < \theta \leq \Delta_2 \alpha \\ sin(\alpha_i - \theta) & \theta > \Delta_2 \alpha \end{cases} \qquad (2)$$

where α = arctan (B/H), α_i = angle between R_i and vertical line through O (Figure 2a), and Δ_1 and Δ_2 non-dimensional parameters defining the three-branches law in Figure 2c, calibrated on experimental tests (Sorrentino, Alshawa, and Liberatore 2014). The hinge O is indented with respect to the geometric corner of the wall by a quantity, u, depending on the masonry design compressive strength, $f_{m,d}$, equal to:

$$u = \frac{m\, g}{2 \cdot 0.85\, f_{m,d} L_h} \qquad (3)$$

where L_h = hinge length, coincident with the wall length if no openings are present. In Eq. (3) a stress block distribution of amplitude 0.85 $f_{m,d}$ has been assumed, as customary in ultimate verifications. Nonetheless, linear distributions have been assumed in the literature for similar cases (Munari et al. 2010). As a consequence of Eq. (3), the following relation holds:

$$\alpha_i = \arctan\left(\frac{B - 2u}{H}\right) \qquad (4)$$

The tie is assumed to stay always horizontal although its wall anchor position *A* (Figure 2b) is updated during the analysis, accounting for finite displacements. The tie contribution is determined by the following parameters: F_y = yield force of the tie, R_t = distance between wall anchor and *O* (Figure 2a), χ = tie non-dimensional force (Figure 3), equal to

$$\chi = \begin{cases} 0 & \varepsilon_t \leq \varepsilon_r \\ 1 + \dfrac{\varepsilon_t - \varepsilon_{max}}{\varepsilon_y} & \varepsilon_r < \varepsilon_t \leq \varepsilon_{max} \\ 1 & \varepsilon_{max} < \varepsilon_t \leq \varepsilon_u \\ 0 & \varepsilon_t > \varepsilon_u \end{cases} \tag{5}$$

ε_t = tie axial deformation, equal to:

$$\varepsilon_t = \varepsilon_y \frac{F_0}{F_y} + 2\frac{R_t}{L_t} cos\left(\alpha_t + \frac{\theta}{2}\right) sin\frac{\theta}{2} \tag{6}$$

where F_0 = prestress force of the tie, L_t = initial length of the tie, α_t= angle between R_t and vertical line through *O* (Figure 2a), ε_y = yield deformation of the steel, ε_{max} = maximum deformation reached so far in the time history, $\varepsilon_r = \varepsilon_{max} - \varepsilon_y$, residual deformation reached so far in the time history, ε_u = ultimate deformation of the steel.

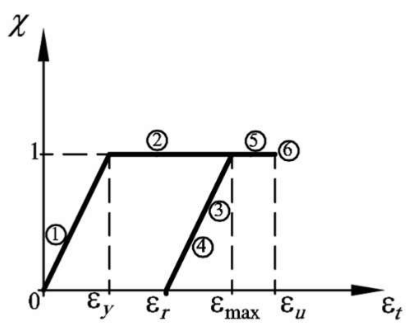

Figure 3. Tie cyclic non-dimensional force - deformation law.

The tie non-dimensional force, χ, introduces an additional source of non-linearity because the tie is not active if a previous permanent deformation is not recovered or if it fails. When the tie fails a sudden release of elastic potential energy occurs. If the wall anchor is bilaterally connected to the façade and the failure occurs close to the anchor, so that no whiplash effect is involved, the potential energy transforms itself in a kinetic energy contribution that gives to the wall an additional angular velocity, $\dot{\theta}_f$, equal to:

$$\dot{\theta}_f = f_{y,d}\sqrt{\frac{A_t L_t}{E_s I_O}} \tag{7}$$

where $f_{y,\,d}$ = steel yield design strength, A_t = tie cross section area, E_s = steel Young's modulus. Because wall anchors are usually just adjacent to the façade, involving a monolateral connection, and the tie failure occurs frequently away from the wall, hereinafter when the tie fails its contribution will be neglected without modifying the wall angular velocity.

During the time history, when the rotation becomes zero the wall hits the base and the transversal structures. At this time an energy dissipation occurs, by means of a negative velocity reduction coefficient. The minus sign involves a rebound, hence keeping rotations positive. The value of the velocity reduction coefficient, also known as coefficient of restitution, has been determined following the conservation of angular momentum approach proposed by Housner (1963) for two-sided rocking, and for one-sided rocking is equal to:

$$e_{an,1s} = 1.05\left(1 - 2\frac{m{R_i}^2}{I_O}\sin^2\alpha_i\right)^2\left(1 - 2\frac{m{R_i}^2}{I_O}\cos^2\alpha_i\right) \tag{8}$$

valid for a generic geometry. The 1.05 coefficient was experimentally calibrated in Sorrentino, AlShawa, and Decanini (2011).

3 PARAMETRIC ANALYSIS

3.1 *Tie code design*

As customary in the Italian technical literature (Giuffrè 1993; Cangi, Caraboni, and De Maria 2010; Munari et al. 2010), the tie is designed according to a force-based procedure lately based on the Commentary to the Italian Building Code (CMIT 2009), so as to have the following horizontal collapse load multiplier:

$$\alpha_0 = \frac{a_g S\, CF\, e^*}{q} \tag{9}$$

where a_g = maximum ground acceleration expected for the life safety limit state in a horizontal rock site, S = site response coefficient (depending on topographic and stratigraphic conditions), CF = confidence factor, e^* = participating mass factor (assumed equal to 1 in the case of a monolithic wall, according to the Italian procedure (Sorrentino et al. 2017)), q = behaviour factor (assumed equal to 2 according to the Commentary to the Italian Building Code (CMIT 2009)).

The tie force, F_y, granting the load multiplier α_0 is equal to

$$F_y = \frac{m\, g(\alpha_0 H - B + 2u)}{2H_t} \tag{10}$$

where H_t = tie force lever arm at rest (Figure 2a). The consequent tie cross section area, A_t, is equal to:

$$A_t = \frac{F_y}{f_{y,d}} \tag{11}$$

In the following, yield design strength has been computed for a partial safety factor larger than one, because the tie is a new element. However, in the technical literature other authors assume a unity value (Munari et al. 2010; Cangi, Caraboni, and De Maria 2010). This issue can be properly resolved only within a fully probabilistic calibration analysis, which is outside the scope of this paper.

In a real case design, the cross section area A_t would be rounded up to account for commercial rod diameters. However, such rounding up would involve a unsystematic effect on the parametric analyses performed hereinafter, also because the assumed unity wall length implicates small tie rod section areas. Therefore, in the following, the cross section area has been simply computed according to Eq. (11).

Code design has been always performed assuming a modern steel S235 as specified in the Italian Building Code (DMI 2008) or in Eurocode 3 (EC3-1-1 2005), and with all relevant values summarised in Table 1. Once the geometry of the tie rod was defined, only a single investigated parameter (pertaining masonry geometry, tie-rod geometry and steel mechanical characteristics) has been changed according to the ranges specified in the following sections, whereas all other parameters are kept constant for all analyses.

Table 1. Assumed values for tie code design

Parameter	Symbol	Value	Unit of measure
Earthquake return period	T_R	500	years
Peak ground acceleration on stiff ground type	a_g	0.26	g
Site response coefficient	S	1.33	-
Confidence factor	CF	1.00	-
Modal participation factor	e^*	1.0	-
Masonry bulk specific weight	w	20	kN/m^3
Masonry design compressive strength	$f_{m,d}$	125	N/cm^2
Wall length	L	1.0	m
Tie rod normalised length	L_t / B	10	-
Tie rod normalised prestress force	F_0 / F_y	0.1	-
Steel Young's modulus	E_s	210	GPa
Steel partial safety coefficient	γ_{m0}	1.05	-
Steel characteristic yield strength	$f_{y,k}$	235	MPa
Steel ultimate elongation	ε_u	0.20	-

3.2 *Historical tie characteristics*

In the previous section the tie has been designed assuming a modern steel, which may have different strengths but usually have unique elastic modulus and ultimate elongation. On the contrary, historical ties display rather different properties, as determined by Calderini et al. (2016). Based on experimental tests performed on a set of tie rods recovered from restoration works or building demolitions, the authors present mean and standard deviation of elastic modulus, yield strength, and ultimate elongation summarised in Table 2. Such values will be the base for the parametric analyses developed in Sect. 4.2 and Sect. 4.3.

Table 2. Mean and standard deviation of Young's modulus, yield strength and ultimate elongation of historical tie rods (Calderini et al. 2016)

	E_s	f_y	ε_u
	GPa	MPa	-
μ	209	218	0.169
σ	76.1	46.1	0.091

3.3 *Ground motion records*

The dynamic model defined in Sect. 2 is investigated under natural records consistent with site-specific and return-period-specific spectral shapes. The site considered is L'Aquila, Southern Italy, for a ground type C according to Eurocode 8 (EC8-1 2004). Three event return periods have been considered: 50, 500 and 1000 years, approximately corresponding to damage limitation, life safety and collapse prevention limit states of ordinary buildings (DMI 2008). The 500 years return period is considered as the most significant and systematically investigated, whereas the 50 and 1000 years return periods are taken into account for comparison purposes only.

In order to increase efficiency and sufficiency of record selection for a system that has an amplitude-dependant vibration period, spectral compliance is pursued in terms of log-average spectral acceleration over the period range 0.1-2.0 s (Kohrangi et al. 2017). Three sets of 40 records each have been used, entailing different accelerograms selected within the RINTC project (Iervolino, Spillatura, and Bazzurro 2017).

The peak ground acceleration and Housner Intensity (Housner 1952) of the records are presented in Figure 4. Peak ground acceleration is relevant for mechanism activation (Housner 1963), whereas Housner Intensity is well correlated with mechanism failure (Marotta et al. 2018). Given the asymmetry of the mechanism under consideration, with rotation allowed only on one side due to the presence of transversal structures, the records are considered with both positive and negative polarity, thus obtaining 80 records.

4 ANALYSES RESULTS

4.1 *Tie effectiveness and role of wall geometry*

Role of wall geometry is emphasised in Figure 5. Four walls have been selected, having height/thickness ratio equal to 8 and 12, and thickness equal to 0.6 and 0.9 m. Therefore, it will be possible to observe the role of aspect ratio as well as that of scale. Geometry has been selected using mean, μ, and standard deviation, σ, values of a population of about 300 masonry walls belonging to ordinary buildings surveyed in Abruzzi region in Southern Italy (Sorrentino 2014), where the wall may span over several floors and the thickness is that at ground floor. Height/thickness ratio values are approximately equal to corresponding $\mu - \sigma$ and μ values, respectively. No larger values have been assumed because they may involve a change of mechanism, from one-body cantilever wall to two-body vertical spanning wall (Penner and Elwood 2016; Abrams et al. 2017). Wall thickness values are approximately equal to corresponding $\mu - \sigma$ and $\mu + \sigma$ values respectively, thus covering a sufficiently ample range.

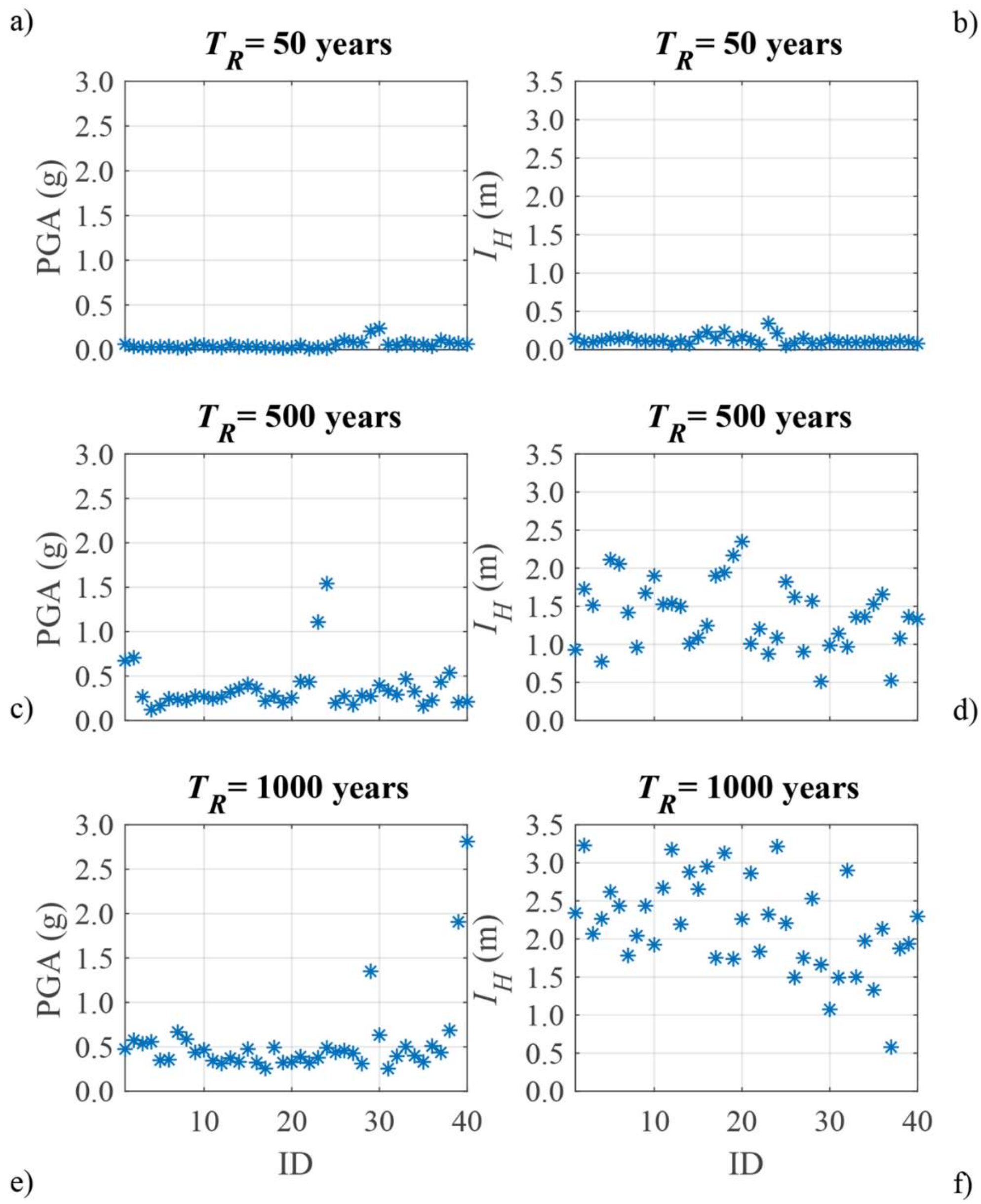

Figure 4. Peak ground acceleration and Housner Intensity of selected records. Return period of the earthquake = a-b) 50 years, c-d) 500 years, e-f) 1000 years.

In Figure 5, the normalised maximum rotation, θ_{max} / α_i, of a façade with no tie rod and with tie rod varying its normalised height, H_t / H (Figure 2a) is plotted. Each marker in the subplots is related to one of the assumed 80 records. For each response it is annotated whether the tie remains elastic or becomes plastic. No failure of the tie has been observed, thus proving the code approach to be safe. The median, the mean and the 90th percentile of the 80 time histories normalised maximum rotations are computed. In the case of the wall without tie rods, median normalised maximum rotation varies between 0.24 and 0.68, whereas mean value varies between 0.31 and 0.67. Hence, a skewness is present in the sample and computing the mean is on the safe side. The range of values is rather ample as an effect of aspect ratio (the lower the height/thickness ratio the smaller the rotation) and scale (the larger the thickness the smaller the rotation). The 90th percentile varies between 0.61 and 1.00.

If similar statistics are computed for the tied walls, much lower values can be observed. Median varies 0.08 and 0.16, mean between 0.12 and 0.20, 90th percentile between 0.27 and 0.49. Hence, ties are rather effective, confirming what found in static analyses by Casapulla et al. (2016). It is worth mentioning that, as an effect of the intervention, the range of variation is much smaller than for the unrestrained wall but wall geometry still plays a role despite tie presence. On one hand, the effect of aspect ratio is negligible: two walls having the same size and different height/thickness ratios have similar responses (in Figure 5 compare a with b, c with d). Although the response of untied walls is influenced by aspect ratio, the analyses show that in tied walls tie cross section (larger for more slender walls) compensates the effect of aspect ratio. On the other hand, walls of same height/thickness ratio but different size experience different maximum rotations (in Figure 5 compare a with c, b with d), a point further discussed in Sect. 4.4. Finally, the height position of the tie rod, thanks to compensating cross section area, has a negligible effect on all considered statistics but the role of tie characteristics is discussed in detail in the following section.

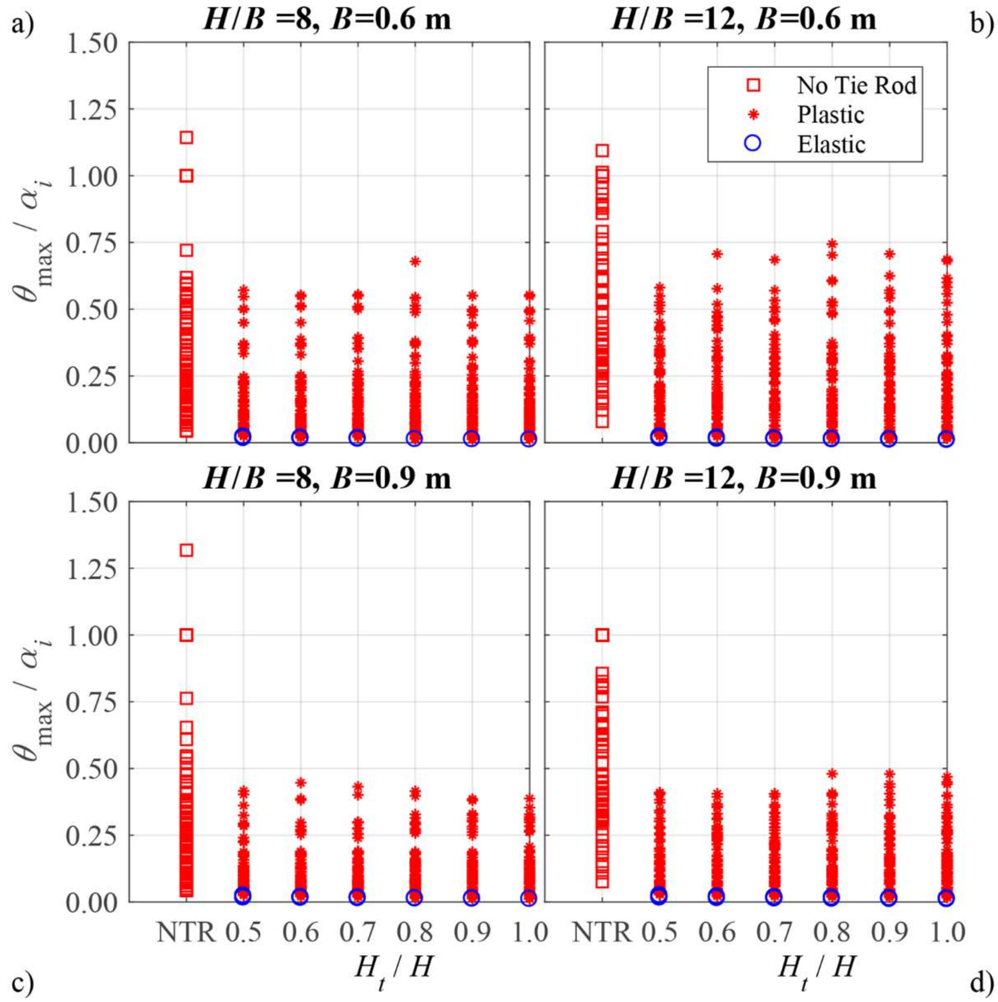

Figure 5. Normalised maximum rotation, θ_{max}/α_i, of a façade with no tie rod and with tie rod varying its normalised height, H_t/H (Figure 2a), and wall geometry (a-d). Assumed values for tie code design as in Table 1. Each marker related to one of the assumed 80 records (40 records with positive and negative polarity). Elastic or plastic response of the tie emphasised. Return period of assumed earthquake T_R = 500 years.

4.2 *Role of tie characteristics*

The role of tie geometry can be investigated in Figure 6, where it is summarised in terms of 90th percentile of maximum normalised rotation. If the size of the cross section area is designed according to the code, hence varying with tie rod position along the wall height (H_t / H), the maximum rotation experienced by the wall is similar in each considered wall and all ties become plastic, a condition emphasised with a letter P above each bar of the plot. In the same Figure, the role of the non-dimensional length of the tie rod, L_t / B, has been investigated. No survey data were found about such parameter, hence values between 4 and 20 have been assumed as rather wide but still reasonable.

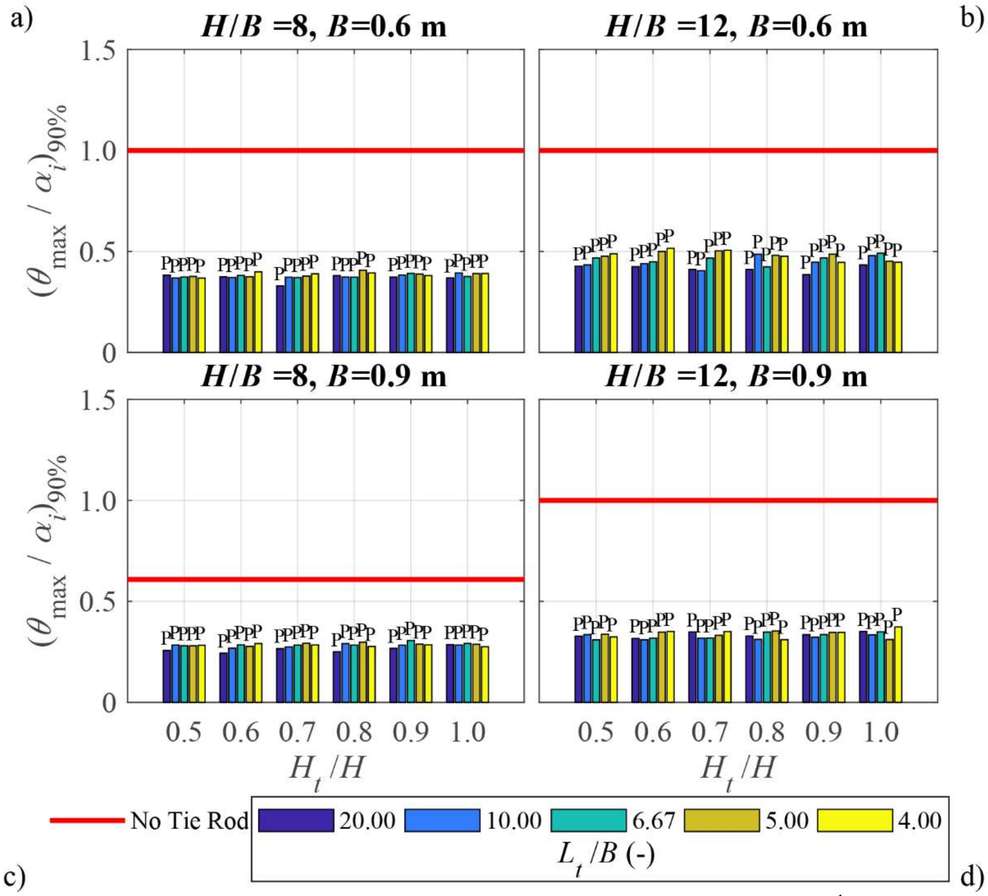

Figure 6. Role of normalised length of the tie rod, L_t/B. Response in terms of the 90th percentile of normalised maximum rotation, θ_{max}/α_i, varying tie rod normalised height, H_t/H (Figure 2a), and wall geometry (a-d). Plastic response of the tie emphasised with a letter P above the bars in the plot. Assumed values for tie code design as in Table 1.

The tie rod length influences the tie rod stiffness and the ultimate elongation. However, no tie rod fails, hence only the effect on stiffness is relevant in the investigated wall geometries. Shorter tie rods are stiffer but present a smaller yield displacement and become plastic before longer ties (Figure 7 - Figure 8). During load reversal the tie is inactive until the permanent deformation is not recovered, and the wall can be substantially rotated when the next significant ground motion pulse occurs. Hence, shorter tie rods tend to be associated with slightly larger maximum rotations. Nonetheless, the overall effect of tie rod length is rather limited.

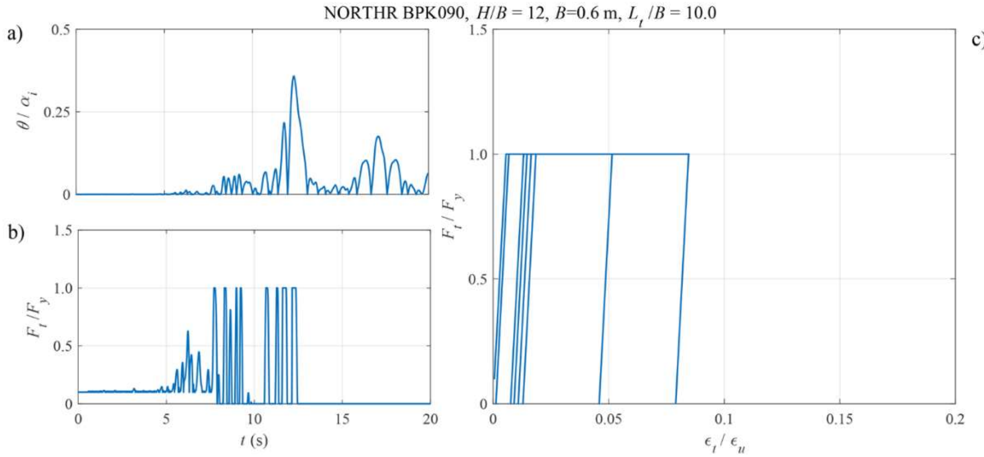

Figure 7. Role of normalised length, $L_t /B = 10.0$. a) time history of normalised rotation, b) time history of tie normalised axial force, c) normalised axial force – elongation. Plot c) starts from prestress elongation.

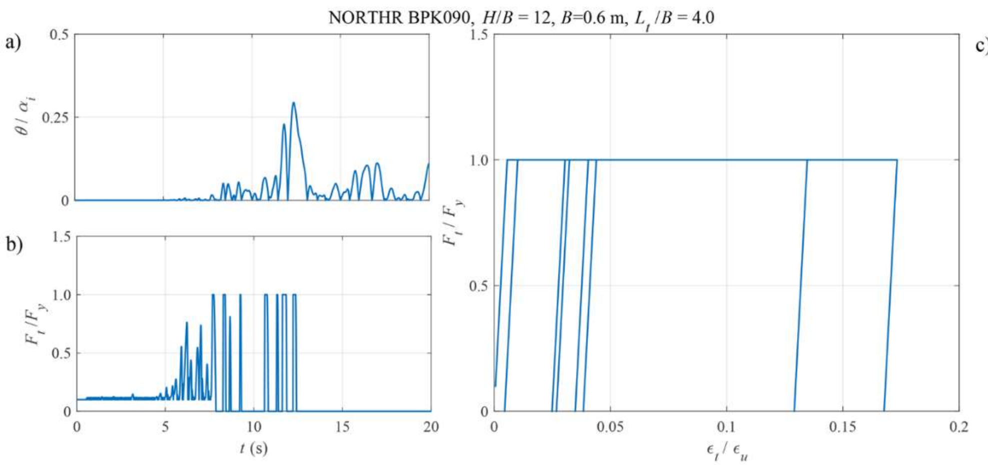

Figure 8. Role of normalised length, $L_t /B = 4.0$. a) time history of normalised rotation, b) time history of tie normalised axial force, c) normalised axial force – elongation.

In Figure 9 the role of prestress force is investigated. In the technical literature there are no established recommended values. Dolce et al. (2006) suggest a tensile prestress in the cross section approximately equal to 10 MPa. Podestà (2012) presents design examples with a prestress in the range 38-113 MPa. Lagomarsino and Calderini (2005) found in the ties of three buildings values in the 32-129 MPa range, which would involve a prestress normalised over average yield strength in Calderini et al. (2016) in the range 0.15-0.59. Rainieri et al. (2015) found in another building normalised prestress in the range 0.16-0.23. Consequently, for the parametric analysis a reasonable range 0.0-0.6 was assumed, comprising the lack of any prestress as well as rather large forces at wall anchor. The overall effect of prestress force is negligible and without systematic trends, even though a normalised prestress as large as 0.80 is assumed (not shown for the sake of brevity). This behaviour can be explained with all ties becoming plastic. However, for 50 years return period earthquakes (corresponding to damage limitation state of ordinary buildings) the ties remain elastic, a condition emphasised with a letter E above each bar of the plot, and a higher prestress reduces rotation amplitude (Figure 10). Nonetheless, differences are rather small and the use of large prestress forces, possibly involving damage at wall anchor already when the intervention is carried out, is questionable. Therefore, the field investigation of the tie rod current stress state seems to be of limited interest.

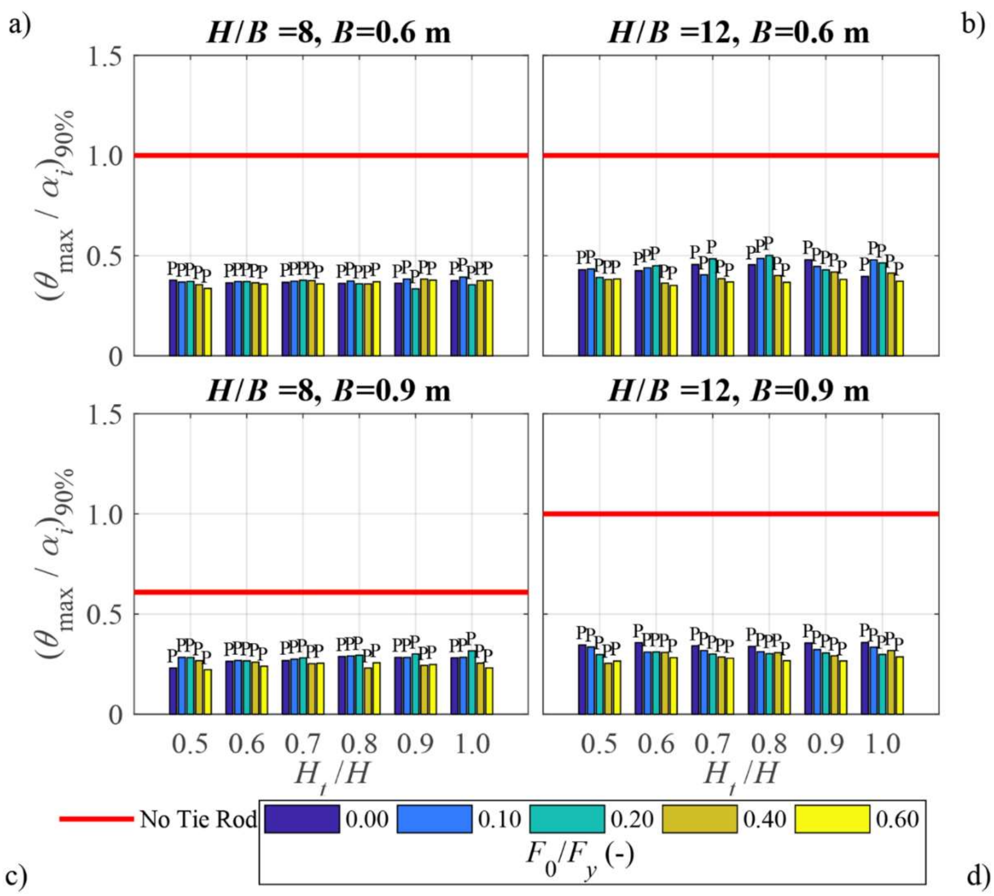

Figure 9. Role of normalised prestress force, F_0/F_y. Response in terms of the 90th percentile of normalised maximum rotation, θ_{max}/α_i, varying tie rod normalised height, H_t/H (Figure 2a), and wall geometry (a-d). Plastic response of the tie emphasised with a letter P above the bars in the plot. Assumed values for tie code design as in Table 1.

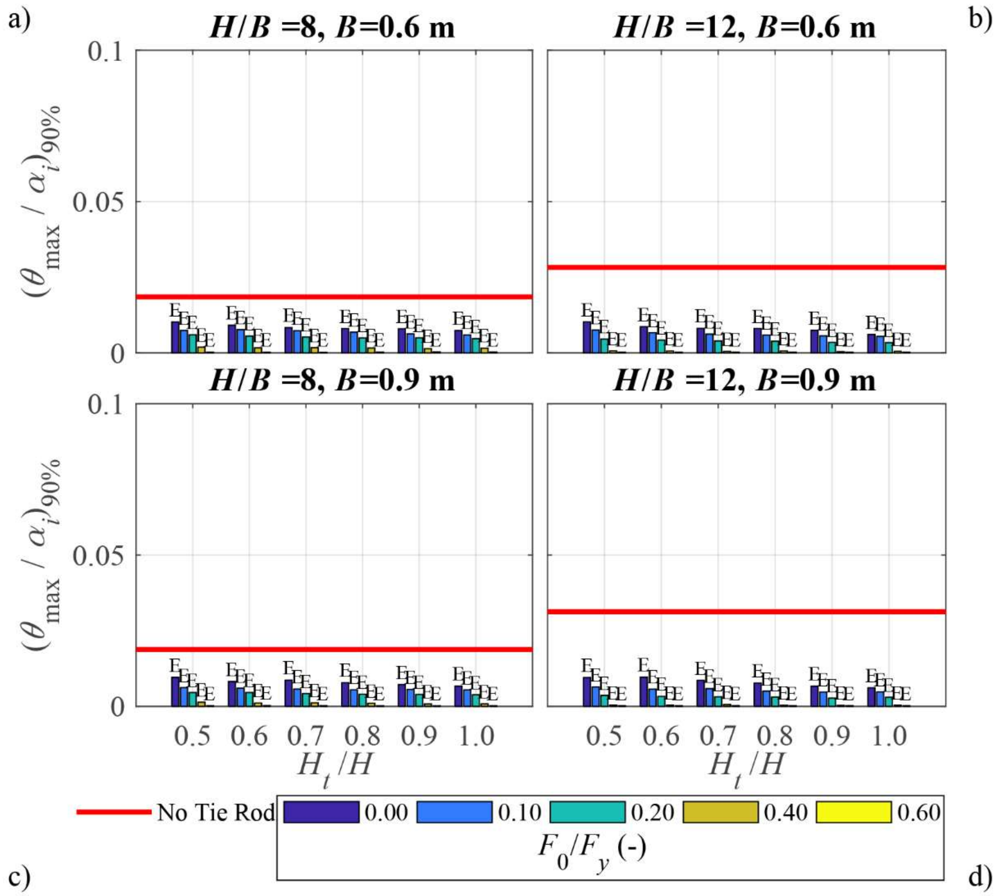

Figure 10. Role of normalised prestress force, F_0/F_y. Response in terms of the 90th percentile of normalised maximum rotation, θ_{max}/α_i, varying tie rod normalised height, H_t/H (Figure 2a), and wall geometry (a-d). Elastic response of the tie emphasised with a letter E above the bars in the plot. Assumed values for tie code design as in Table 1, but record selection according to an earthquake return period T_R = 50 years.

4.3 *Role of steel characteristics*

The role of Young's modulus is analysed in Figure 11, wherein the range of values is that derived from mean, μ, and standard deviation, σ, values in Table 2, thus assuming $E_s = \mu \pm 1.64\sigma$, $\mu \pm \sigma$, μ. It is worth mentioning that the mean value of this range is rather similar to the codified value assumed for the design tie rod in Table 1. The effect of an increased Young's modulus is limited and similar to that of a shorter tie, already discussed in Figure 6. Hence, an increased maximum rotation can be observed, at least at life safety limit state. At damage limitation limit state no tie becomes plastic, hence the stiffer tie rod involves smaller rotations but again with rather negligible differences (not shown for the sake of conciseness). Similar results, again not shown for the sake of brevity, were obtained varying the tie rod axial stiffness.

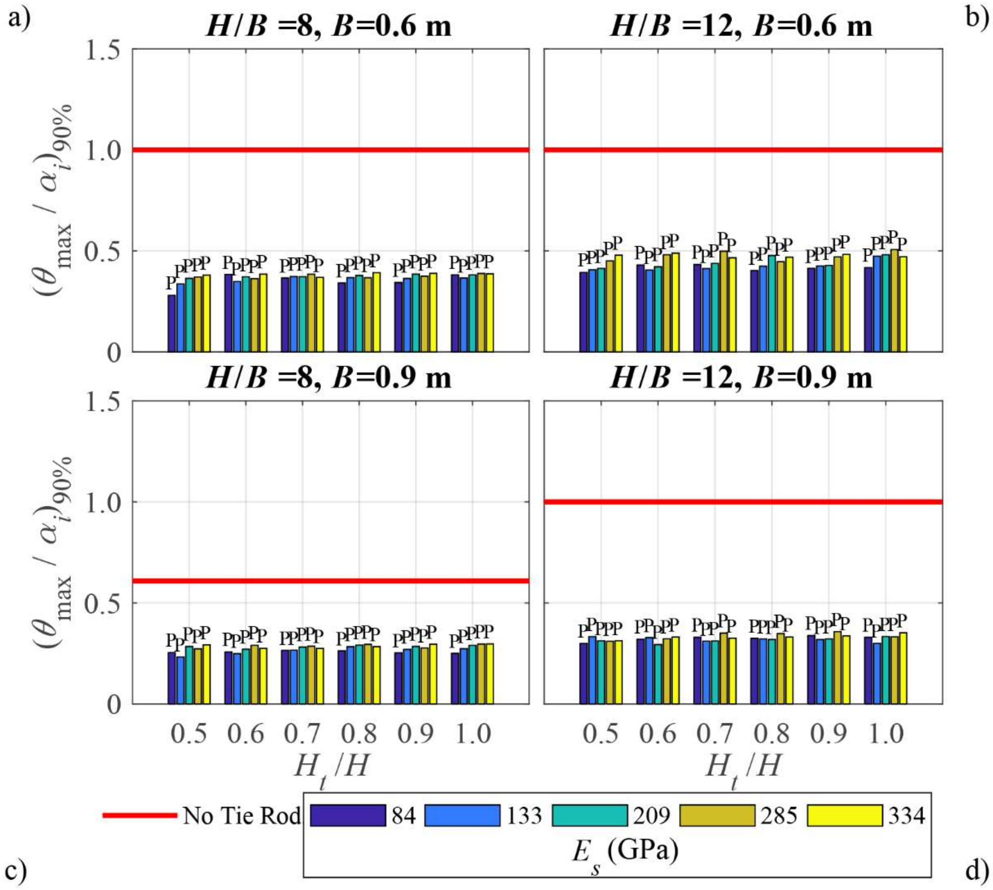

Figure 11. Role of steel Young's modulus, E_s. Response in terms of the 90[th] percentile of normalised maximum rotation, θ_{max}/α_i, varying tie rod normalised height, H_t/H (Figure 2a), and wall geometry (a-d). Plastic response of the tie emphasised with a letter P above the bars in the plot. Assumed values for tie code design as in Table 1.

Yield strength is studied in Figure 12, wherein varies according to mean and standard deviation values in Table 2, thus assuming $f_{y,d} = \mu \pm 1.64\sigma$, $\mu \pm \sigma$, μ, with mean value rather close to the codified design value. It is important to reiterate that the ties are designed according to the code procedure described in Sect. 3.2, hence walls of given geometry and tie-rod position share the same tie-rod cross section, same Young's modulus, same prestress force, as well as all other parameters, and in the parametric analyses only yield strength varies. Consequently, yield force and yield displacement increase with increasing yield strength and, conversely, experienced maximum rotation reduces. All this considered, yield strength is the most relevant parameter and influences the response, as one could expect. Steel strength can be estimated by means of correlation with hardness tests (Gaško and Rosenberg 2011; Pavlina and Vantyne 2008), for which field procedures have been proposed (Haggag 2001; Mehdianpour and Waßmuth 2016), although so far not on tie rods.

a)

b)

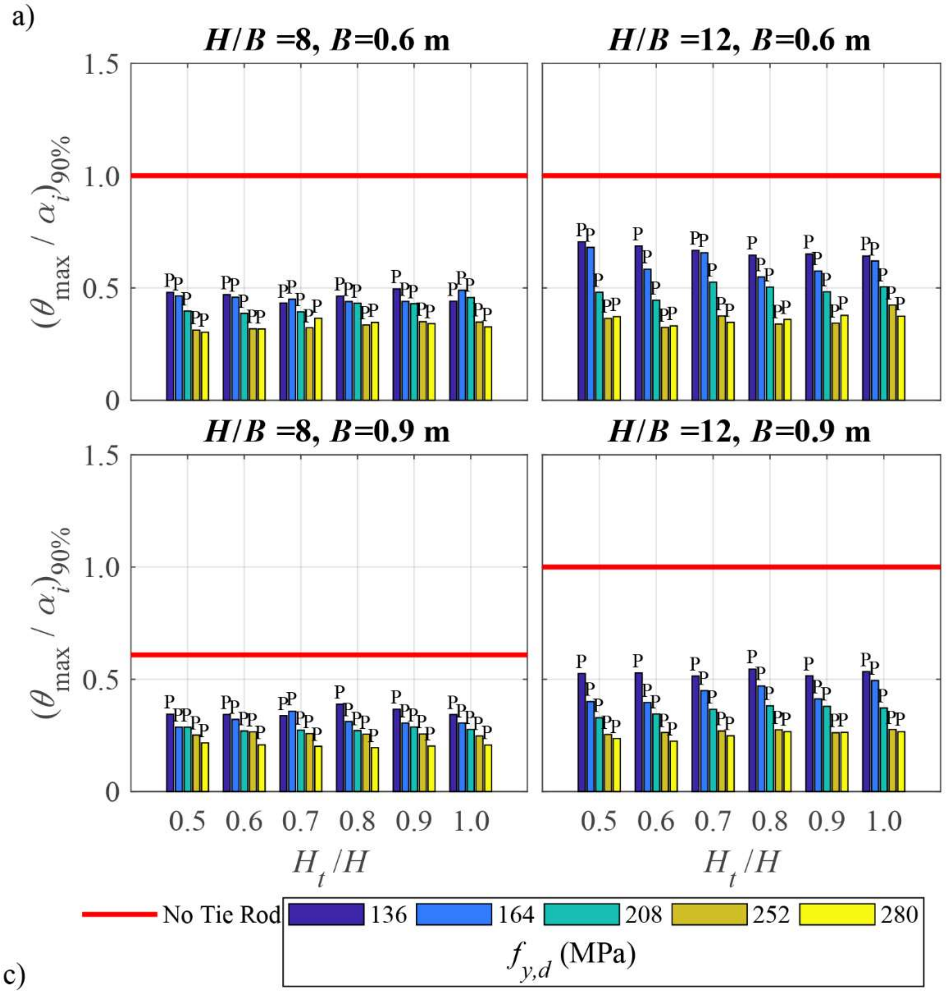

c)

d)

Figure 12. Role of yield strength, f_y. Response in terms of the 90th percentile of normalised maximum rotation, θ_{max}/α_i, varying tie rod normalised height, H_t/H (Figure 2a), and wall geometry (a-d). Plastic response of the tie emphasised with a letter P above the bars in the plot. Assumed values for tie code design as in Table 1.

Considering the great relevance that displacement-based procedures have gained in earthquake engineering it is worth studying the role of the ultimate elongation (Figure 13). This parameter varies according to mean and standard deviation values in Table 2, thus assuming $\varepsilon_u = \mu \pm 1.64\sigma$, $\mu \pm \sigma$, μ, with mean value rather close to the codified design value. Surprisingly, there is a very limited effect of ultimate elongation on the response and tie failures, a condition emphasised with a letter F above relevant bars of the plot, occur only for very low (and unlikely) ultimate elongation values. Of course, ultimate displacement is a function of ultimate elongation and tie rod initial length that, because normalised by wall thickness, involves a higher relevance of ultimate elongation for thinner walls and for rods located at higher positions where displacement is larger. All this considered, the analyses have been repeated halving the normalised length (L_t / B = 5) but the differences are limited (Figure 14). Only very short normalised length (L_t / B = 2, not shown for the sake of conciseness) can induce some failures for an elongation equal to 0.08, which is still a rather conservative value within historical values although approximately equal to codified elongation of concrete rebars (DMI 2008). Hence, at least for investigated wall geometries and tie rod lengths, the ultimate elongation is not a crucial parameter and force-based design is acceptable.

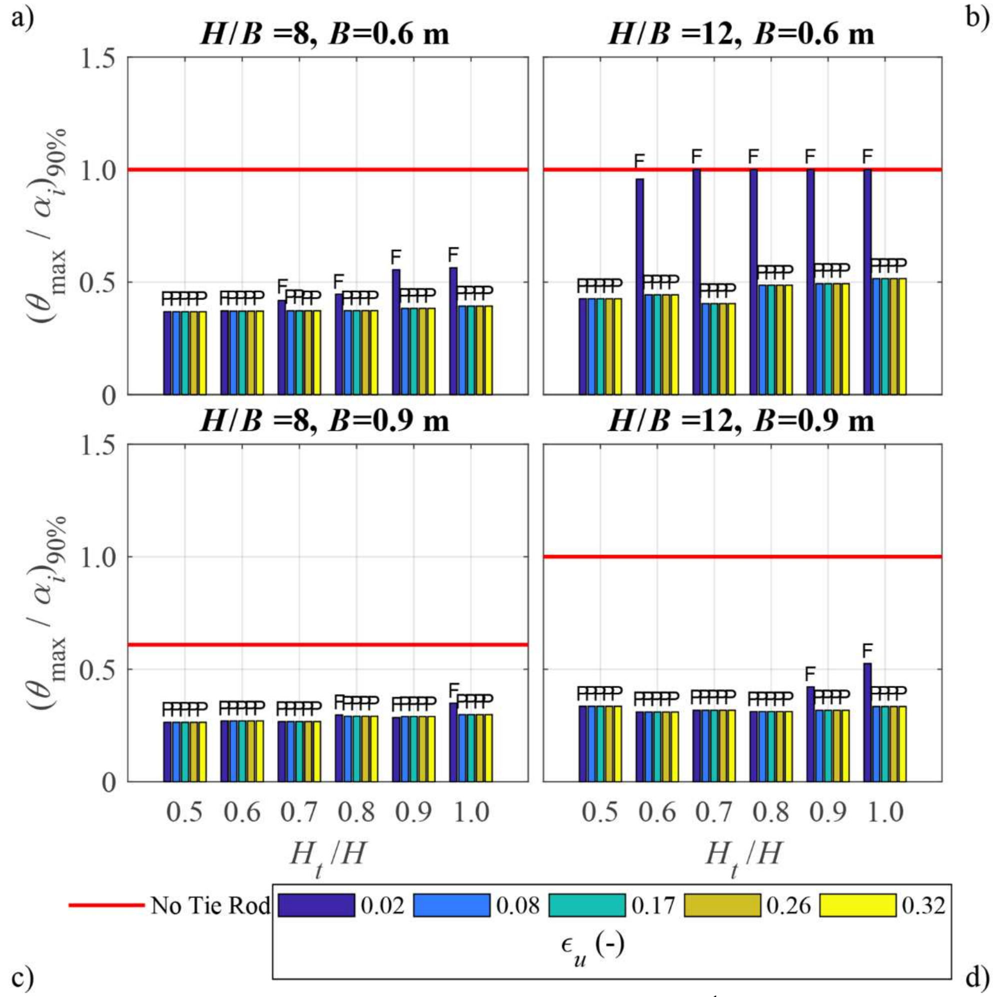

Figure 13. Role of ultimate elongation, ε_u. Response in terms of the 90[th] percentile of normalised maximum rotation, θ_{max}/α_i, varying tie rod normalised height, H_t/H (Figure 2a), and wall geometry (a-d). Plastic or failed response of the tie emphasised with a letter P or F, respectively, above the bars in the plot. Assumed values for tie code design as in Table 1. Normalised tie rod length $L_t/B = 10$.

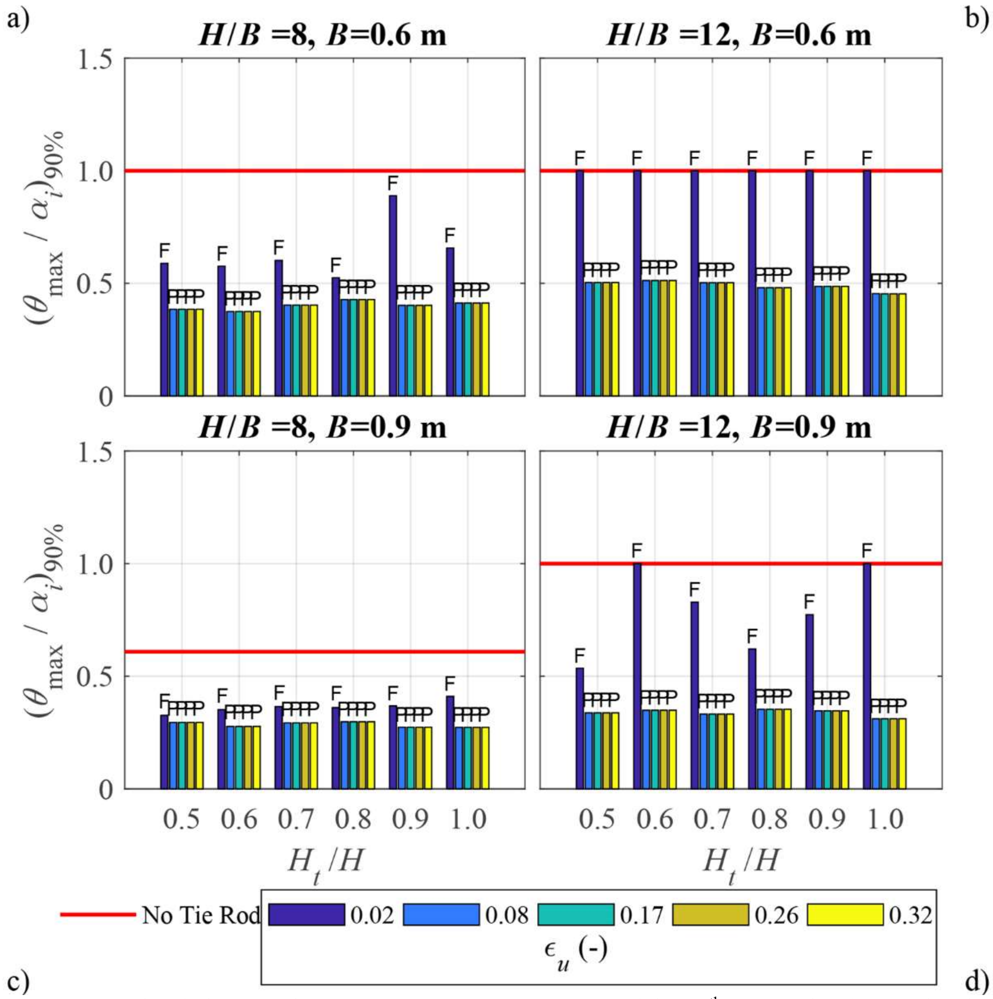

Figure 14. Role of ultimate elongation, ε_u. Response in terms of the 90th percentile of normalised maximum rotation, θ_{max}/α_i, varying tie rod normalised height, H_t/H (Figure 2a), and wall geometry (a-d). Plastic or failed response of the tie emphasised with a letter P or F, respectively, above the bars in the plot. Assumed values for tie code design as in Table 1. Normalised tie rod length L_t /B = 5.

4.4 *Code considerations*

In Figure 5 it was shown that a force-based tie design according to the Commentary to the Italian Building Code (CMIT 2009) is rather effective when compared to the same walls without ties. According to the Commentary, at life safety limit state (static) demand / capacity ratio should not exceed 0.40, unless horizontal-structures collapse occurs for smaller displacements. It was shown in Figure 5 that median, over 80 time histories, of normalised maximum rotation varies between 0.08 and 0.16, mean between 0.12 and 0.20, 90th percentile between 0.27 and 0.49. Hence, code recommendations are certainly met.

Nonetheless, variation in safety level is substantial because the force-design procedure described in Sect. 3.1, is not capable to account for the size of the wall, the well-known scale effect (Housner 1963). This behaviour is related to the different contribution in terms of potential energy that the tie designed according to strength can deliver to walls of same height/thickness ratio but different size.

Assimilating for the sake of brevity the wall without tie rod to a rectangular block, the potential energy with respect to centroid position is equal to:

$$V_W = mgR_i[cos(\alpha_i - \theta) - cos\alpha_i] \tag{12}$$

Excluding previous plastic cycles, the potential energy of the tie rod is equal to:

$$V_{TR} = \frac{1}{2}E_s A_t L_t \begin{cases} \varepsilon_t^2 & \varepsilon_t \leq \varepsilon_y \\ \varepsilon_y^2 & \varepsilon_y < \varepsilon_t \leq \varepsilon_u \\ 0 & \varepsilon_t > \varepsilon_u \end{cases} \tag{13}$$

In Figure 15 the potential energy of the wall restrained by tie rods is normalised by that of the unrestrained wall, in order to emphasise the role of the tie. It is evident that walls having the same aspect ratio have almost coincident potential ratio, irrespective of the tie rod vertical position. On the contrary, if the size of the wall is changed a difference can be observed in the potential energy ratio. Hence, alternative procedures such as displacement- or energy-based (Sorrentino et al. 2017) should be explored, although they may involve a more convoluted design process for the practitioners.

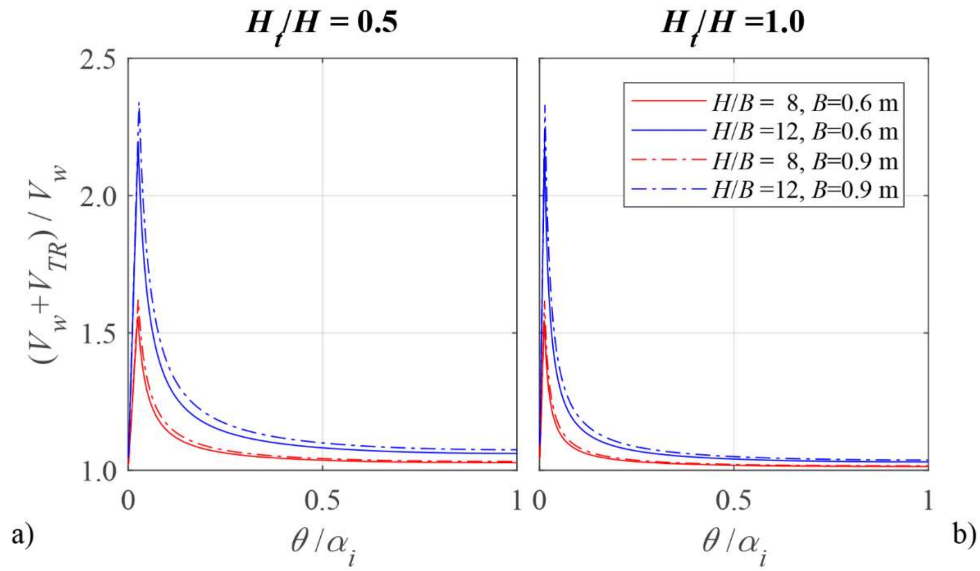

Figure 15. Potential energy of the wall restrained by tie rods ($V_W + V_{TR}$), normalised by that of the unrestrained wall (V_W) varying wall geometry and hinge position. No previous plastic cycle.

The previous analyses have been repeated assuming an earthquake with return period T_R = 1000 years that, according to the Italian building code (DMI 2008), can be approximately related to the collapse prevention limit state of an ordinary building (Figure 16). For the unrestrained wall the median of the normalised maximum rotation varies between 0.74 and 1.00, mean between 0.69 and 0.92, 90th percentile is equal to 1.00 (overturning) for all geometries. It is worth mentioning that no value larger than 1.00 (overturning) is possible by default, thus explaining why median is larger than mean. For the tied walls the median varies between 0.35 and 0.66, mean between 0.40 and 0.70, 90th percentile between 0.70 and 1.25. In this case the 1.00 threshold is exceeded because of the presence of an elongated tie. Reported statistics should be compared with a larger normalised rotation than for the life safety limit state. An Eurocode draft under preparation (Lu et al. 2016) assumes for the collapse prevention limit state a (static) θ_{max} / α_i = 0.60. Hence, current code procedure seems to involve a reasonable protection against collapse, although probably not as large as desirable. Failures of tie rods can be observed in some instances and a conventional normalised maximum rotation equal to unity has been plotted. Contrary to Figure 13 and Figure 14, in these plots tie failure always involves wall overturning, therefore pushover analyses (Lagomarsino 2015; Cangi, Caraboni, and De Maria 2010; Podestà 2012) should probably neglect the curve beyond tie crisis.

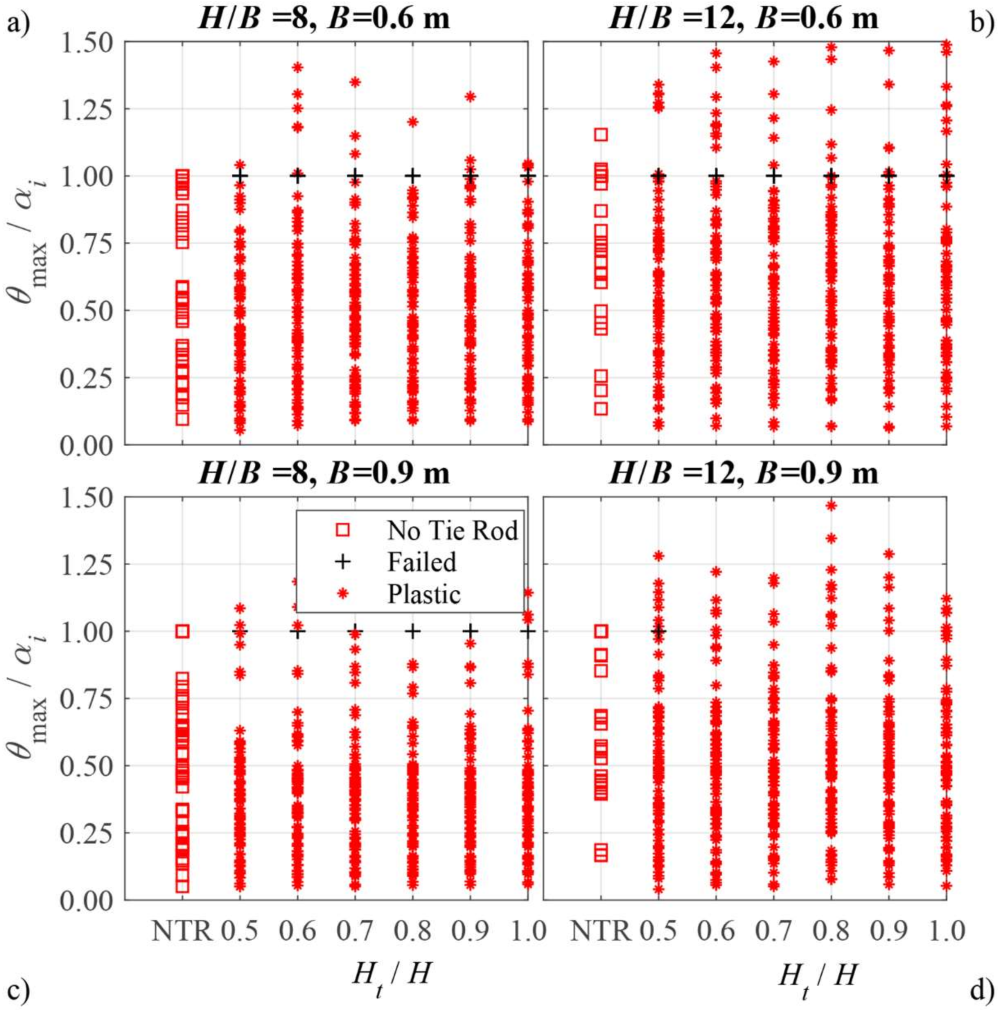

Figure 16. Normalised maximum rotation, $\theta_{\max}/\alpha_i$, of a façade with no tie rod and with tie rod varying its normalised height, H_t/H (Figure 2a), and wall geometry (a-d). Assumed values for tie code design as in Table 1. Each marker related to one of the assumed 80 records (40 records with positive and negative polarity). Plastic or failed response of the tie emphasised. Failed response involves overturning, with a conventional normalised maximum rotation equal to unity. Record selection according to an earthquake return period T_R = 1000 years.

The design performed in Sect. 3.1 assumed a behaviour factor q = 2 in Eq. (9), as recommended in the Italian procedure (CMIT 2009). In Figure 17 analyses are repeated, for 500 years earthquake records, assuming for design q = 1. Median of normalised maximum rotation becomes now as low as 0.01-0.02, mean 0.03-0.04, 90th percentile 0.09-0.15. Hence, such behaviour factor involves rather conservative results. In Figure 18 analyses are repeated assuming for design q = 3. Median of normalised maximum rotation becomes now as high as 0.17-0.31, mean

0.21-0.38, 90th percentile 0.41-0.81. For this behaviour factor failures of tie rods can be observed even for 500 years return period earthquake records, which is probably unacceptable.

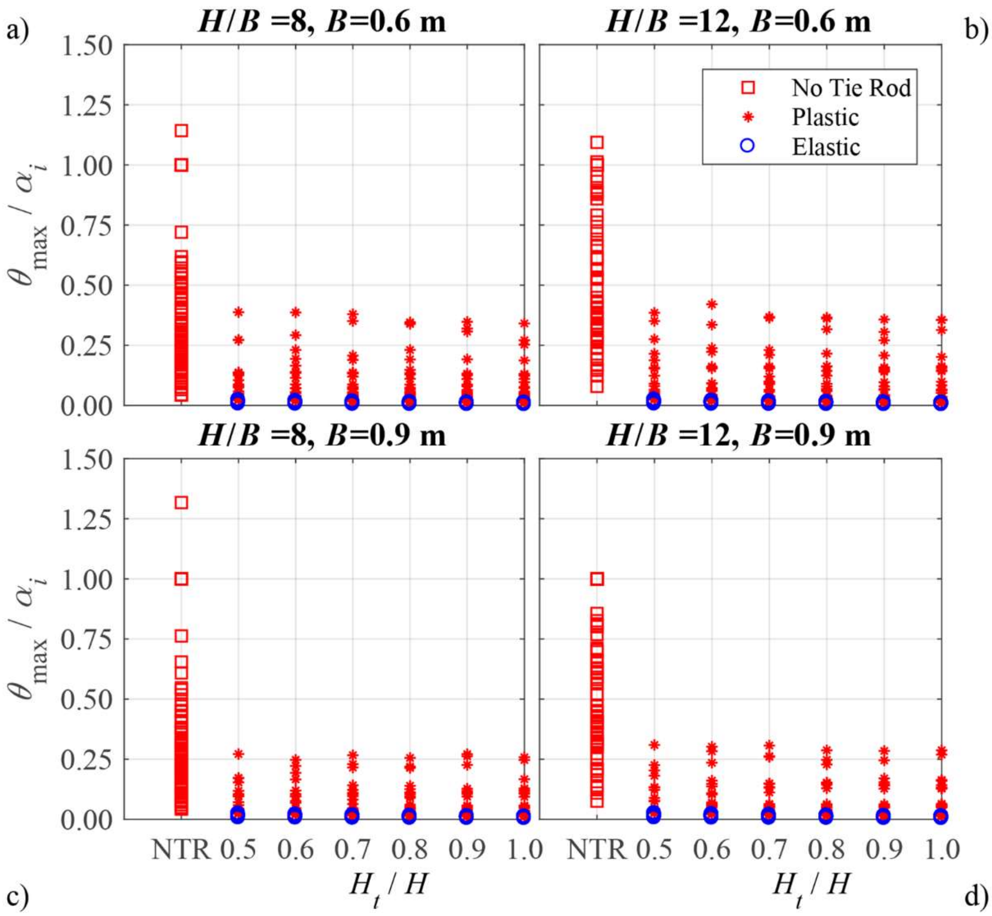

Figure 17. Normalised maximum rotation, $\theta_{\max}/\alpha_i$, of a façade with no tie rod and with tie rod varying its normalised height, H_t/H (Figure 2a), and wall geometry (a-d). Each marker related to one of the assumed 80 records (40 records with positive and negative polarity). Elastic or plastic response of the tie emphasised. Assumed values for tie code design as in Table 1, with the exception of behaviour factor $q = 1$.

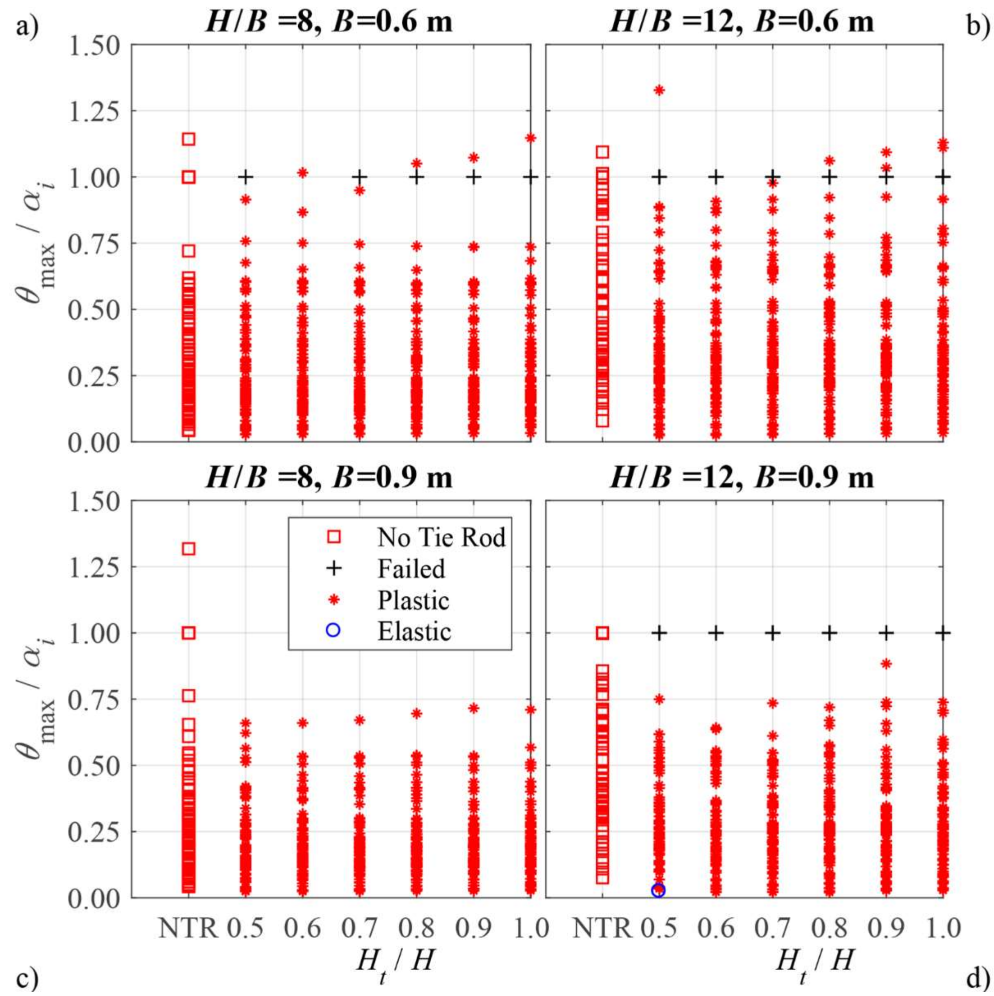

Figure 18. Normalised maximum rotation, $\theta_{\max}/\alpha_i$, of a façade with no tie rod and with tie rod varying its normalised height, H_t/H (Figure 2a), and wall geometry (a-d). Each marker related to one of the assumed 80 records (40 records with positive and negative polarity). Elastic, plastic or failed response of the tie emphasised. Failed response involves overturning, with a conventional normalised maximum rotation equal to unity. Assumed values for tie code design as in Table 1, with the exception of behaviour factor q = 3.

5 CONCLUSIONS

In this paper the non-linear equation of motion of a single-body wall restrained by an elasto-plastic tie rod of finite displacement capacity is proposed. The wall has a flat base and an indented corner pivot about which it can rotate on one side only. The response has two sources of non-linearity, one geometry related and one material related. The material related non-linearity is further complicated by the tie being inactive if a previous permanent deformation is not recovered or if the tie fails.

The tie rod is designed according to the Commentary to the Italian Building Code, following a force-based approach and assuming a modern steel, and the restrained wall is excited by a set natural records. The intervention is rather effective in reducing the wall initial vulnerability, whatever the vertical position of the tie. The code procedure assumes a behaviour factor $q = 2$, a value that guarantees substantial protection both at life safety limit state and some protection at collapse prevention limit state. On the contrary, a unity value would involve a rather conservative design and $q = 3$ induces larger rotations and a few failures already for 500 years return period earthquakes, failures that are not present for lower values of behaviour factor. Unfortunately, the force-based procedure is unable to capture the different safety levels of two walls of same height/thickness ratio but different size. Therefore, in the future displacement- or energy-based procedures could be investigated.

Tie rods are not a recent technique because they were used extensively in the past. Therefore, it is useful to investigate whether historical iron/steel can prove as effective as modern steel by means of a parametric analysis. First of all, tie rod geometry has been defined according to a modern design, then a single parameter at time has been changed. Meaningful ranges of iron/steel characteristics are assumed from experimental literature on historical specimens.

The role of Young's modulus is very limited both at life safety and damage limitation limit states and the same applies to the tie rod length, which affects stiffness. Similarly, ultimate elongation is relevant only if very low and unlikely values are assumed. Therefore, force-based procedures prove to be at the same time effective and easy to implement. Yield strength is much more relevant and specific non-destructive techniques, possibly based on measurement of hardness, should be specifically developed for steel tie rods. Non-destructive techniques already exist to estimate prestress that, however, shows little relevance for both ultimate and serviceability limit states. Therefore, large pretensioning forces should be avoided in new interventions, in order to avert masonry damage at wall anchor. Wall anchor failures and the formation of intermediate hinge were excluded in this analysis, but need to be properly investigated in future studies.

AKNOWLEDGEMENTS

This work has been partially carried out under the programs "Dipartimento della Protezione Civile – Consorzio RELUIS", Research Line Masonry structures. The opinions expressed in this publication are those of the authors and are not necessarily endorsed by the Dipartimento della Protezione Civile.

REFERENCES

Abrams, D.P., O. AlShawa, P.B. Lourenço, and L. Sorrentino. 2017. "Out-of-Plane Seismic Response of Unreinforced Masonry Walls: Conceptual Discussion, Research Needs, and Modeling Issues." *International Journal of Architectural Heritage* 11 (1): 22–30. doi:10.1080/15583058.2016.1238977.

AlShawa, O., L. Sorrentino, and D. Liberatore. 2017. "Simulation Of Shake Table Tests on Out-of-Plane Masonry Buildings. Part (II): Combined Finite-Discrete Elements." *International Journal of Architectural Heritage* 11 (1): 79–93. doi:10.1080/15583058.2016.1237588.

Andreotti, C., D. Liberatore, and L. Sorrentino. 2015. "Identifying Seismic Local Collapse Mechanisms in Unreinforced Masonry Buildings through 3D Laser Scanning." *Key Engineering Materials* 628: 79–84. doi:10.4028/www.scientific.net/KEM.628.79.

Brando, G., D. Rapone, E. Spacone, M.S. O'Banion, M.J. Olsen, A.R. Barbosa, M. Faggella, et al. 2018. "Damage Reconnaissance of Unreinforced Masonry Bearing Wall Buildings after the 2015 Gorkha, Nepal, Earthquake." *Earthquake Spectra*. doi:10.1193/010817EQS009M.

Bruneau, M. 1994. "State-of-the-Art Report on Seismic Performance of Unreinforced Masonry Buildings." *Journal of Structural Engineering (United States)* 120 (1): 230–251. doi:10.1061/(ASCE)0733-9445(1994)120:1(230).

Calderini, C., R. Vecchiattini, C. Battini, and P. Piccardo. 2016. "Mechanical and Metallographic Characterization of Iron Tie-Rods in Masonry Buildings: An Experimental Study." In *Structural Analysis of Historical Constructions: Anamnesis, Diagnosis, Therapy, Controls - Proceedings of the 10th*

International Conference on Structural Analysis of Historical Constructions, SAHC 2016, 1293–1300.

Campbell, J, D. Dizhur, M. Hodgson, G. Ferguson, and J. Ingham. 2012. "Test Results for Extracted Wall-Diaphragm Anchors from Christchurch Unreinforced Masonry Buildings." *Journal of the Structural Engineering Society of New Zealand* 25 (1): 56–67.

Cangi, G., M. Caraboni, and A. De Maria. 2010. *Analisi Strutturale per Il Recupero Antisismico: Calcolo Dei Cinematismi per Edifici in Muratura Secondo Le NTC*. Roma: DEI.

Casapulla, C., L.U. Argiento, F. Da Porto, and D. Bonaldo. 2016. "The Relevance of Frictional Resistances in out-of-Plane Mechanisms of Block Masonry Structures." In *Brick and Block Masonry: Trends, Innovations and Challenges - Proceedings of the 16th International Brick and Block Masonry Conference, IBMAC 2016*, 119–128.

Celik, O.C., H. Sesigur, and F. Cili. 2009. "Importance of Wood and Iron Tension Members on Seismic Performance of Historic Masonry Buildings: Three Case Studies from Turkey." In *Improving the Seismic Performance of Existing Buildings and Other Structures*, 1374–1383. doi:10.1061/41084(364)126.

CMIT. 2009. *Circolare Del Ministro Delle Infrastrutture E Dei Trasporti 2 Febbraio 2009, N. 617, Contenente Le Istruzioni per L'applicazione Delle "Nuove Norme Tecniche per Le Costruzioni" Di Cui Al DM 14 Gennaio 2008*. Gazzetta Ufficiale della Repubblica Italiana n. 47 del 26 febbraio 2009, Supplemento Ordinario n. 27.

De Felice, G. 2011. "Out-of-Plane Seismic Capacity of Masonry Depending on Wall Section Morphology." *International Journal of Architectural Heritage* 5 (4–5): 466–482. doi:10.1080/15583058.2010.530339.

Degli Abbati, S., S. Cattari, I. Marassi, and S. Lagomarsino. 2015. *Seismic out-of-Plane Assessment of Podestà Palace in Mantua (Italy)*. *Key Engineering Materials*. Vol. 624. doi:10.4028/www.scientific.net/KEM.624.88.

Dimitrakopoulos, E.G., and M.J. DeJong. 2012. "Overturning of Retrofitted Rocking Structures under Pulse-Type Excitations." *Journal of Engineering Mechanics* 138 (8): 963–972. doi:10.1061/(ASCE)EM.1943-7889.0000410.

DMI. 2008. *Decreto Del Ministro Delle Infrastrutture 14 Gennaio 2008. Approvazione Delle Nuove Norme Tecniche per Le Costruzioni*. Gazzetta Ufficiale della Repubblica Italiana, n. 29 del 4 febbraio 2008, Supplemento Ordinario n. 30.

Dolce, M, D Liberatore, C Moroni, G Perillo, G Spera, and A Cacosso. 2006. *Manuale Delle Opere Provvisionali Urgenti Post-Sisma*. Potenza.

EC3-1-1. 2005. *Eurocode 3: Design of Steel Structures - Part 1-1: General Rules and Rules for Buildings*. *Eurocode 3*. Brussels: European Committee for Standardization.

EC8-1. 2004. *Eurocode 8: Design of Structures for Earthquake resistance—Part 1: General Rules, Seismic Actions and Rules for Buildings*. Brussels: European Committee for Standardization.

Gaško, Martin, and Gejza Rosenberg. 2011. "Correlation between Hardness and Tensile Properties in Ultra-High Strength Dual Phase Steels – Short Communication." *Materials Engineering* 18 (4): 155–159.

Giresini, L., M. Fragiacomo, and P.B. Lourenço. 2015. "Comparison between Rocking Analysis and Kinematic Analysis for the Dynamic out-of-Plane Behavior of Masonry Walls." *Earthquake Engineering and Structural Dynamics* 44 (13): 2359–2376. doi:10.1002/eqe.2592.

Giuffrè, A. 1993. *Sicurezza E Conservazione Dei Centri Storici: Il Caso Ortigia*. Roma-Bari: Laterza.

Gizzi, F T, N Masini, M Sileo, C Zotta, M Scavone, M R Potenza, D Liberatore, L Sorrentino, and M Bruno. 2014. "Building Features and Safeguard of Church Towers in Basilicata (Southern Italy)." In *2nd International Congress on Science and Technology for the Conservation of Cultural Heritage*, 369–374.

Haggag, F. 2001. *In-Situ Nondestructive Measurements of Key Mechanical Properties of Oil and Gas Pipelines*. *American Society of Mechanical Engineers, Pressure Vessels and Piping Division (Publication) PVP*. Vol. 429.

Housner, G.W. 1952. "Spectrum Intensities of Strong Motion Earthquakes." In *Proceedings of the Symposium of Earthquake and Blast Effects on Structures, EERI, Los Angeles, California,* 21–36.

Housner, G W. 1963. "The Behavior of Inverted Pendulum Structures during Earthquakes." *Bulletin of the Seismological Society of America* 53 (2): 403–417.

Iervolino, I., A. Spillatura, and P. Bazzurro. 2017. "RINTC Project: Assessing the (Implicit) Seismic Risk of Code-Conforming Structures in Italy." In *6thECCOMAS Thematic Conference on Computational Methods in Structural Dynamics and Earthquake Engineering, Rhodes, Greece, 15– 17 June*. doi:10.7712/120117.5512.17282.

Indirli, M., and M.G. Castellano. 2008. "Shape Memory Alloy Devices for the Structural Improvement of Masonry Heritage Structures." *International Journal of Architectural Heritage* 2 (2): 93–119. doi:10.1080/15583050701636258.

Kohrangi, M., P. Bazzurro, D. Vamvatsikos, and A. Spillatura. 2017. "Conditional Spectrum-Based Ground Motion Record Selection Using Average Spectral Acceleration." *Earthquake Engineering and Structural Dynamics* 46 (10): 1667–1685. doi:10.1002/eqe.2876.

Lagomarsino, S. 2015. “Seismic Assessment of Rocking Masonry Structures.” *Bulletin of Earthquake Engineering* 13 (1): 97–128. doi:10.1007/s10518-014-9609-x.

Lagomarsino, S., and C. Calderini. 2005. “The Dynamical Identification of the Tensile Force in Ancient Tie-Rods.” *Engineering Structures* 27 (6): 846–856. doi:10.1016/j.engstruct.2005.01.008.

Liberatore, D, N Masini, L Sorrentino, V Racina, M Sileo, O AlShawa, and L Frezza. 2016. “Static Penetration Test for Historical Masonry Mortar.” *Construction and Building Materials*, no. 122: 810–822. doi:10.1016/j.conbuildmat.2016.07.097.

Lu, S., K. Beyer, V. Bosiljkov, C. Butenweg, D. D’Ayala, H. Degee, M. Gams, et al. 2016. “Next Generation of Eurocode 8, Masonry Chapter.” In *Brick and Block Masonry: Trends, Innovations and Challenges - Proceedings of the 16th International Brick and Block Masonry Conference, IBMAC 2016*.

Lucibello, G., G. Brandonisio, E. Mele, and A. De Luca. 2013. “Seismic Damage and Performance of Palazzo Centi after L’Aquila Earthquake: A Paradigmatic Case Study of Effectiveness of Mechanical Steel Ties.” *Engineering Failure Analysis* 34: 407–430. doi:10.1016/j.engfailanal.2013.09.011.

Magenes, G., A. Penna, I. Senaldi, M. Rota, and A. Galasco. 2014. “Shaking Table Test of a Strengthened Full-Scale Stone Masonry Building with Flexible Diaphragms.” *International Journal of Architectural Heritage* 8 (3): 349–375. doi:10.1080/15583058.2013.826299.

Makris, N, and J Zhang. 2001. “Rocking Response of Anchored Blocks under Pulse-Type Motions.” *Journal of Engineering Mechanics* 127 (5): 484–493. doi:10.1061/(ASCE)0733-9399(2001)127:5(484).

Marotta, A., L. Sorrentino, D. Liberatore, and J.M. Ingham. 2018. “Seismic Risk Assessment of New Zealand Unreinforced Masonry Churches Using Statistical Procedures.” *International Journal of Architectural Heritage* 12 (3): 448–464. doi:10.1080/15583058.2017.1323242.

Marotta, A, T Goded, S Giovinazzi, S Lagomarsino, D Liberatore, L Sorrentino, and J M Ingham. 2015. “An Inventory of Unreinforced Masonry Churches in New Zealand.” *Bulletin of the New Zealand Society for Earthquake Engineering* 48 (3): 171–190.

Mehdianpour, M., and C.-F. Waßmuth. 2016. “Minimally Invasive Material Tests on Guyed Tubular Masts | Minimalinvasive Materialuntersuchungen an Seilabgespannten Rohrmasten Zur Bauwerkserhaltung.” *Bautechnik*. doi:10.1002/bate.201500094.

Mendes, N., A.A. Costa, P.B. Lourenço, R. Bento, K. Beyer, G. de Felice, M. Gams, et al. 2017. “Methods and Approaches for Blind Test Predictions of Out-of-Plane Behavior of Masonry Walls: A Numerical Comparative Study.” *International Journal of Architectural Heritage* 11 (1): 59–71.

doi:10.1080/15583058.2016.1238974.

Moon, L., D. Dizhur, I. Senaldi, H. Derakhshan, M. Griffith, G. Magenes, and J. Ingham. 2014. "The Demise of the URM Building Stock in Christchurch during the 2010-2011 Canterbury Earthquake Sequence." *Earthquake Spectra*. doi:10.1193/022113EQS044M.

Munari, M., G. Bettiol, F. da Porto, L. Milano, and C. Modena. 2010. *Esempio Di Calcolo Su Rafforzamento Locale Di Edifici in Muratura Con Tiranti. Allegato Alle Linee Guida per La Riparazione E Il Rafforzamento Di Elementi Strutturali, Tamponature E Partizioni*. Napoli.

Paret, T.F., S.A. Freeman, G.R. Searer, M. Hachem, and U.M. Gilmartin. 2008. "Using Traditional and Innovative Approaches in the Seismic Evaluation and Strengthening of a Historic Unreinforced Masonry Synagogue." *Engineering Structures* 30 (8): 2114–2126. doi:10.1016/j.engstruct.2007.03.023.

Pavlina, E J, and Chester Vantyne. 2008. "Correlation of Yield Strength and Tensile Strength with Hardness for Steels." *Journal of Materials Engineering and Performance* 17 (December): 888–893. doi:10.1007/s11665-008-9225-5.

Penna, A., I. E. Senaldi, A. Galasco, and G. Magenes. 2016. "Numerical Simulation of Shaking Table Tests on Full-Scale Stone Masonry Buildings." *International Journal of Architectural Heritage* 10 (2–3): 146–163. doi:10.1080/15583058.2015.1113338.

Penner, O., and J.E. Elwood. 2016. "Out-of-Plane Dynamic Stability of Unreinforced Masonry Walls in One-Way Bending: Shake Table Testing." *Earthquake Spectra* 32 (3): 1675–1697.

Podestà, S. 2012. *Verifica Sismica Di Edifici in Muratura: Aggiornato a NTC E Linee Guida per La Valutazione E Riduzione Della Vulnerabilità Sismica*. Palermo: Dario Flaccovio.

Pomonis, A., and M. Gaspari. 2014. "Earthquake Loss Estimation and Benefit-Cost Analysis of Mitigation Measures for Buildings in Greece: Case Study of Pylos Town." *Bollettino Di Geofisica Teorica Ed Applicata* 55 (2): 535–560. doi:10.4430/bgta0072.

Prajapati, S., O. AlShawa, and L. Sorrentino. 2015. "Out-of-Plane Behaviour of Single-Body Unreinforced-Masonry Wall Restrained by a Flexible Diaphragm." In *COMPDYN 2015 - 5th ECCOMAS Thematic Conference on Computational Methods in Structural Dynamics and Earthquake Engineering*, 3127–3138. National Technical University of Athens.

Rainieri, C., A. Marra, G.M. Rainieri, D. Gargaro, M. Pepe, and G. Fabbrocino. 2015. "Integrated Non-Destructive Assessment of Relevant Structural Elements of an Italian Heritage Site: The Carthusian Monastery of Trisulti." *Journal of Physics: Conference Series* 628 (1): 12018. doi:10.1088/1742-

6596/628/1/012018.

Rosenboom, O.A., S.J. Kelley, and T.F. Paret. 2014. "Rehabilitation of Maison Dufort: Adopting Traditional Techniques for Seismic Retrofitting." In *10th U.S. National Conference on Earthquake Engineering: Frontiers of Earthquake Engineering, July 21-25, Anchorage, Alaska*, 1043. doi:10.4231/D3FJ29D4G.

Sorrentino, L. 2014. "Reconstruction Plans After the 2009 L'Aquila Earthquake. From Building Performance to Historical Centre Performance." In *9th International Conference on Structural Analysis of Historical Constructions, Mexico City, 14–17 October*, 11–006.

Sorrentino, L., O. AlShawa, and L.D. Decanini. 2011. "The Relevance of Energy Damping in Unreinforced Masonry Rocking Mechanisms. Experimental and Analytic Investigations." *Bulletin of Earthquake Engineering* 9 (5): 1617–1642. doi:10.1007/s10518-011-9291-1.

Sorrentino, L., O. Alshawa, and D. Liberatore. 2014. "Observations of out-of-Plane Rocking in the Oratory of San Giuseppe Dei Minimi during the 2009 L'Aquila Earthquake." *Applied Mechanics and Materials* 621. Trans Tech Publications Ltd: 101–106. doi:10.4028/www.scientific.net/AMM.621.101.

Sorrentino, L., D. D'Ayala, G. de Felice, M.C. Griffith, S. Lagomarsino, and G. Magenes. 2017. "Review of Out-of-Plane Seismic Assessment Techniques Applied To Existing Masonry Buildings." *International Journal of Architectural Heritage* 11 (1): 2–21. doi:10.1080/15583058.2016.1237586.

Sorrentino, L, D Bruccoleri, and M Antonini. 2008. "Structural Interpretation of Post-Earthquake (19th Century) Retrofitting on the Santa Maria Degli Angeli Basilica, Assisi, Italy." *6th International Conference On Structural Analysis of Historic Construction* 2008: 217.

Tomaževič, M., M. Lutman, and P. Weiss. 1996. "Seismic Upgrading of Old Brick-Masonry Urban Houses: Tying of Walls with Steel Ties." *Earthquake Spectra* 12 (3): 599–622. doi:10.1193/1.1585898.

Walsh, K. Q., D. Y. Dizhur, N. Almesfer, P. A. Cummuskey, J. Cousins, H. Derakhshan, M. C. Griffith, and J. M. Ingham. 2014. "Geometric Characterisation and out-of-Plane Seismic Stability of Low-Rise Unreinforced Brick Masonry Buildings in Auckland, New Zealand." *Bulletin of the New Zealand Society for Earthquake Engineering* 47 (2): 139–156.

Zucconi, M., R. Ferlito, and L. Sorrentino. 2017. "Simplified Survey Form of Unreinforced Masonry Buildings Calibrated on Data from the 2009 L'Aquila Earthquake." *Bulletin of Earthquake Engineering*. doi:10.1007/s10518-017-0283-7.

Zucconi, M., L. Sorrentino, and R. Ferlito. 2017. "Principal Component Analysis for a Seismic Usability Model of Unreinforced Masonry Buildings." *Soil Dynamics and Earthquake Engineering* 96: 64–75.

doi:10.1016/j.soildyn.2017.02.014.